



First measurement of the Λ - Ξ interaction in proton-proton collisions at the LHC

ALICE Collaboration*



ARTICLE INFO

Article history:

Received 5 May 2022

Accepted 31 May 2022

Available online 3 June 2022

Editor: M. Pierini

ABSTRACT

The first experimental information on the strong interaction between Λ and Ξ^- strange baryons is presented in this Letter. The correlation function of Λ - Ξ^- and $\bar{\Lambda}$ - Ξ^+ pairs produced in high-multiplicity proton-proton (pp) collisions at $\sqrt{s} = 13$ TeV at the LHC is measured as a function of the relative momentum of the pair. The femtoscopy method is used to calculate the correlation function, which is then compared with theoretical expectations obtained using a meson exchange model, chiral effective field theory, and Lattice QCD calculations close to the physical point. Data support predictions of small scattering parameters while discarding versions with large ones, thus suggesting a weak Λ - Ξ^- interaction. The limited statistical significance of the data does not yet allow one to constrain the effects of coupled channels like Σ - Ξ and N - Ω .

© 2022 European Organization for Nuclear Research, ALICE. Published by Elsevier B.V. This is an open access article under the CC BY license (<http://creativecommons.org/licenses/by/4.0/>). Funded by SCOAP³.

1. Introduction

Understanding the strong interaction among hadrons with strange quarks is one of the main challenges faced by nuclear physics at low energies. Recent theoretical developments, in parallel with the improvement of computing facilities, enabled Lattice QCD calculations close to the physical point for systems rich in strangeness [1–4]. In contrast to other approaches describing hadron-hadron interactions, such first principles calculations become more stable the higher the (quark) masses involved, and they are expected to deliver reliable results for the interaction of hadrons involving several strange quarks. On the experimental side, data are scarce for hadron-hadron interactions in the strangeness $|S| > 1$ sector due to the difficulties of producing hyperons in large amounts and the fact that those are unstable particles. Hence, the interest in this sector resides in delivering precise data in order to test the ab-initio calculations.

The study of baryon-baryon interactions with strangeness is also crucial for the search of possible di-baryon states beyond the deuteron. One debated case is the $N\Omega$ state predicted by Lattice QCD calculations [3] and meson exchange models [5]. It would be held together by an attractive strong interaction at all distances favored by the absence of Pauli blocking in this system. Two-particle correlation studies of p - Ω^- [6,7] show that drawing a firm conclusion on its existence is a difficult task due to the complexity of this system that arises from the coupling to several other channels. It has been demonstrated in Ref. [8] that the presence of

coupled channels modifies the correlation function, in particular in the case of systems size of the order of 1 fm, such as those produced in pp collisions. The thresholds of the Λ - Ξ and the Σ - Ξ channels lie around 180 and 90 MeV/ c^2 below the N - Ω threshold, respectively; the influence of those channels could severely modify the p - Ω^- correlation function [9,10] depending on the coupling strength and the characteristics of the Λ - Ξ and the Σ - Ξ interactions themselves. The investigation of those channels is thus mandatory in order to clarify the existence of the $N\Omega$ bound state.

Besides the first principles calculations, in the sector of nucleon-hyperon (N - Y) and hyperon-hyperon (Y - Y) interactions with strangeness content $|S| \leq 3$, several predictions from different theoretical approaches are waiting for validation since over a decade. Leading order (LO) chiral Effective Field Theory (χ EFT) [11], meson exchange models [12], and quark constituent models [13] produced predictions for the $|S| \leq 2$ sectors relying on SU(3) symmetry considerations. Those approaches were anchored to the vast database available in the N - N sector, which includes precise determination of scattering cross sections that enable differential studies and partial wave analyses, to measurements of Λ - N cross sections and, to a lesser extent, to Σ - N cross sections. Very recently, the extension of NLO χ EFT potentials from $S = -2$ [14,15] to $S = -3$ and $S = -4$ systems has been explored [16]. These potentials are in accordance with the few experimental constraints on the Λ - Λ and Ξ - N interactions and account for effects from SU(3) symmetry breaking in the extension.

At the time when most of those potentials were constructed there was little hope for precise data on the interaction between baryon pairs with more than two strange quarks, and the experi-

* E-mail address: alice-publications@cern.ch.

mental information was limited to the scarce data derived from the detection of hypernuclei, such as binding energies for double- Λ hypernuclei [17–20] and Ξ hypernuclei [21,22]. However, binding energies alone do not allow unambiguous conclusions on the underlying baryon–baryon interactions, and so the available theoretical predictions were awaiting more demanding tests.

Only recently, the femtoscopy technique has delivered precise data with valuable information for the description of the strong interaction among hadrons via the study of two-particle correlations as a function of the relative momentum using collider experiments [23]. Measurements of multi-strange systems Λ - Λ [24–26], p - Ξ^- [27], and p - Ω^- [6,7] have been made available from Au-Au collisions at RHIC by STAR and from pp collisions at the LHC by ALICE.

A pioneering study with the first experimental information of the Λ - Ξ^- interaction is presented in this Letter. This measurement constitutes the first benchmark for models and theoretical approaches delivering predictions for this system.

2. Data analysis

The analysis of the correlation function of Λ - Ξ^- and $\bar{\Lambda}$ - $\bar{\Xi}^+$ pairs is performed in the sample of high-multiplicity pp collisions at $\sqrt{s} = 13$ TeV collected by ALICE [28,29] at the LHC during the Run 2 period. The V0 detector of the ALICE apparatus is used for event selection and triggering. The V0 detector consists of two plastic scintillator arrays located on both sides of the collision vertex at pseudorapidities $2.8 < \eta < 5.1$ and $-3.7 < \eta < -1.7$ [30]. In order to guarantee an uniform acceptance at midrapidity, events are accepted for analysis if the reconstructed primary interaction vertex position along the beam axis (V_z) is located no more than 10 cm away from the nominal interaction point. In addition, a V0-based high-multiplicity trigger is used for selecting events in which the detected signal amplitude exceeds a defined threshold corresponding to the 0.17% highest-multiplicity events out of all inelastic collisions with at least one measured charged particle within $|\eta| < 1$ ($\text{INEL} > 0$). The resulting average charged-particle multiplicity density at midrapidity ($|\eta| < 0.5$) is about $\langle dN_{\text{ch}}/d\eta \rangle = 30$. An enhanced production of hyperons was reported for such high-multiplicity events [31], which provides an abundant sample of hyperons for this analysis.

Strange baryon reconstruction is performed using topological properties of their weak decays, which in turn employs the tracking and particle identification capabilities of the ALICE detector. The Inner Tracking System (ITS) and the Time-Projection Chamber (TPC) are used for charged-particle tracking and momentum reconstruction, the TPC is used as well for particle identification (PID), and the Time-of-Flight detector (TOF) is used for timing information. The ITS, TPC, and TOF are immersed in a uniform magnetic field along the beam direction with a strength of 0.5 T. The ITS [32] is made up of six layers of high position-resolution silicon detectors placed at a radial distance between 3.9 and 43 cm around the beam pipe. The TPC [33] is a 5 m long gaseous cylindrical detector covering the whole azimuth within the pseudorapidity range $|\eta| < 0.9$. It performs PID by measuring the specific energy loss (dE/dx). The TOF [34] consists of Multigap Resistive Plate Chambers which cover the full azimuth range at $|\eta| < 0.9$. Combinatorial background from out-of-bunch collision pile-up in the TPC is suppressed by rejecting charged tracks unless a matched hit in the ITS, which does not have out-of-bunch pile-up, or in the TOF, with timing information, is present.

The Λ ($\bar{\Lambda}$) are identified exploiting their characteristic V-shaped weak decay $\Lambda \rightarrow p + \pi^-$ and $\bar{\Lambda} \rightarrow \bar{p} + \pi^+$, henceforth denoted “ V^0 ” decays, and selected within an invariant mass window of $4 \text{ MeV}/c^2$ around the Λ nominal mass. Proton and pion tracks are reconstructed using the TPC, and they are identified

through the TPC dE/dx measurement. They are further combined into V^0 candidates if a certain pair of proton and pion tracks passes a set of geometrical criteria that ensures their consistency with the desired decay topology. These include a selection on the distance of closest approach (DCA) of the two tracks, the cosine of the pointing angle (CPA) between the line connecting the primary vertex with the candidate's decay vertex and its momentum, and the decay radius. Furthermore, a minimal transverse momentum of $p_T \geq 0.3 \text{ MeV}/c$ is required for the Λ ($\bar{\Lambda}$) candidates.

The Ξ^- ($\bar{\Xi}^+$) candidates are identified via the weak decay channel $\Xi^- \rightarrow \Lambda + \pi^-$ and $\bar{\Xi}^+ \rightarrow \bar{\Lambda} + \pi^+$ by combining V^0 candidates with a third track with a TPC energy loss signature that is consistent with the pion mass hypothesis. They are selected within an invariant mass window of $5 \text{ MeV}/c^2$ around the nominal Ξ^- mass. Also in this case, geometric selections serve to identify the expected trajectory arrangement and include standard Λ and $\bar{\Lambda}$ selections as well as a DCA between the V^0 and the third track and a CPA of the Ξ candidate momentum with respect to the estimated decay position. Also the Ξ^- ($\bar{\Xi}^+$) candidates are required to have a minimal transverse momentum of $p_T \geq 0.3 \text{ MeV}/c$. Candidates are rejected if they are compatible within $5 \text{ MeV}/c^2$ with the Ω^- ($\bar{\Omega}^+$) baryon invariant mass through the weak decay $\Omega^- \rightarrow \Lambda + K^-$ ($\bar{\Omega}^+ \rightarrow \bar{\Lambda} + K^+$) by assuming the kaon mass hypothesis for the third track.

The numerical values of the geometrical variables used to select Λ ($\bar{\Lambda}$) and Ξ^- ($\bar{\Xi}^+$), as well as the variations of such values used to estimate the systematic uncertainties of the data, are based on previous analyses; see Ref. [25] and Ref. [35] for Λ ($\bar{\Lambda}$) and Ξ^- ($\bar{\Xi}^+$), respectively. A fit to the invariant mass spectrum of Λ ($\bar{\Lambda}$) and Ξ^- ($\bar{\Xi}^+$) candidates is performed using a double Gaussian to describe the signal and a first-order polynomial for the combinatorial background. For the calculation of the invariant mass of Λ ($\bar{\Lambda}$) the pion and proton hypothesis are used for the daughter tracks; in the case of Ξ^- ($\bar{\Xi}^+$) the Λ ($\bar{\Lambda}$) mass is used for the V^0 and the pion mass for the charged track. The results of the fit deliver average mass resolutions of around 1.5 and $2 \text{ MeV}/c^2$ and purities of 95% and 92% for Λ ($\bar{\Lambda}$) and Ξ^- ($\bar{\Xi}^+$), respectively.

Events are kept for further analysis if at least one Λ ($\bar{\Lambda}$) and one Ξ^- ($\bar{\Xi}^+$) candidate are reconstructed, which results in a total number of 8.57×10^6 events and 5.08×10^6 (4.75×10^6) Λ - Ξ^- ($\bar{\Lambda}$ - $\bar{\Xi}^+$) pairs.

During the reconstruction, a charged track can be assigned as a decay product of multiple V^0 candidates. For such cases, an additional selection procedure is implemented to reduce the combinatorial background and choose the best candidate in an unbiased way. The V^0 candidates that share a charged track are discriminated by using several kinematic variables simultaneously, namely the invariant mass, the DCA, and the CPA. They are compared to template distributions from Monte Carlo (MC) simulations and normalized by their expected resolution such that they have the same incidence in the comparison. For the MC templates, pp events are generated using PYTHIA 8.2 [36] and the resulting particles are propagated through the simulation of the ALICE detector using GEANT3 [37]. An analogous track cleaning procedure is used as well for the Ξ candidates that share charged tracks. The track cleaning procedure reduces the sample of Ξ^- and $\bar{\Xi}^+$ candidates by 0.6% and the sample of Λ and $\bar{\Lambda}$ candidates by 1.9% .

In order to avoid autocorrelations generated by the pairing of Λ ($\bar{\Lambda}$) candidates with their mother particles, pairs of Λ - Ξ^- ($\bar{\Lambda}$ - $\bar{\Xi}^+$) are not considered if the Λ ($\bar{\Lambda}$) candidate shares any charged track with the Ξ^- ($\bar{\Xi}^+$) candidate.

3. Correlation function

Experimentally, the two-particle correlation function is defined as [38]

$$C(k^*) = \mathcal{N} \times \frac{N_{\text{same}}(k^*)}{N_{\text{mixed}}(k^*)}, \quad (1)$$

where k^* is the relative momentum in the pair rest frame, defined as $k^* = \frac{1}{2} \times |\mathbf{p}_1^* - \mathbf{p}_2^*|$ with \mathbf{p}_i being the three-momenta of the involved particle candidates. The N_{same} is the k^* distribution of particle pairs produced in the same collision, whereas N_{mixed} is the k^* distribution obtained by pairing particles produced in different collisions with similar V_z and multiplicity. Due to the event mixing procedure, the number of pairs in N_{mixed} is higher than in N_{same} , hence the correlation function has to be normalized at large k^* , where the effects of the final state interactions are absent. This is denoted by the factor \mathcal{N} ; the normalization is performed in the region $k^* \in [450, 650]$ MeV/c. In the following, $\Lambda-\Xi^-$ is used to refer to the sum of $\Lambda-\Xi^-$ and $\bar{\Lambda}-\Xi^+$ pairs, since both experience the same interaction and correlation and no significant differences are observed between both pairs during the analysis. A total of 6142 $\Lambda-\Xi^-$ pairs are found with k^* below 200 MeV/c.

On the theoretical side, the correlation function can be expressed as a function of the particle emitting source $S(r^*)$ and the two-particle pair wave function $|\Psi(r^*, k^*)|$ which contains the interaction component [38]

$$C(k^*) = \int d^3r^* S(r^*) |\Psi(r^*, k^*)|^2, \quad (2)$$

where r^* refers to the relative distance between the two particles. The source function is assumed to have a Gaussian shape. Its size is obtained from the universal baryon–baryon transverse mass (m_T) scaling observed in high-multiplicity pp collisions [39], and considering its enlargement due to shortly lived resonances [39]. The average transverse mass of $\Lambda-\Xi^-$ pairs with $k^* < 200$ MeV/c is $\langle m_T \rangle = 2.01$ GeV/c², which leads to an effective source radius of $r_{\text{eff}} = 1.032^{+0.055}_{-0.056}$ fm. The quoted uncertainties take into account the statistical and systematic uncertainties of the parametrization of the m_T dependence [39].

Given the source size, the theoretical correlation function is computed using two different methods. The Lednický–Lyuboshits (LL) approach [40,41] allows one to calculate the theoretical correlation function when the effective range parameters are known: scattering length f_0^s and effective range d_0^s , with s denoting the spin state of the pair. Note that in this Letter the standard notation and sign convention in femtoscopy is used, where a positive f_0 corresponds to an attractive interaction, while a negative scattering length corresponds either to a repulsive potential or a bound state. For $\Lambda-\Xi^-$ pairs, there are two spin configurations, namely a singlet with $s=0$ and a triplet with $s=1$. They contribute with a weight of 1/4 and 3/4 to the total theoretical correlation function, respectively. The LL model is used to evaluate the predictions from the Nijmegen meson exchange model [12] and the interactions from χ EFT [11,16]. The second method uses the CATS framework [42], a Schrödinger equation solver, to evaluate the wave functions for the potentials extracted from Lattice QCD calculations performed by the HAL QCD Collaboration [2].

The $\Lambda-\Xi^-$ correlation functions evaluated for the central value of the radius r_{eff} for each considered theoretical prediction are shown in Fig. 1. Since the Coulomb interaction is absent, the deviations from unity at small relative momentum are exclusively due to the strong interaction. Details on the characteristics of each interaction are discussed in Section 4.

The experimental correlation function contains additional contributions to the genuine $\Lambda-\Xi^-$ strong interaction as it is defined

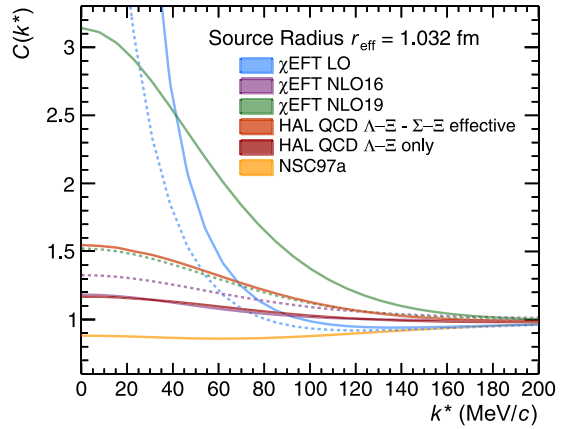


Fig. 1. Theoretical $\Lambda-\Xi^-$ correlation functions from predictions ([2,11,12,16]) evaluated for the experimental source radius. See text for details. In the case of the LO and NLO χ EFT potentials the solid (dotted) lines correspond to the lowest (highest) cutoff [11,16].

in Eq. 2. In order to compare the theoretical expectations with the experimental data, a model is built for each theoretical prediction containing all contributions to the experimental correlation function as detected by ALICE

$$C_{\text{model}}(k^*) = C_{\text{non-femto}}(k^*) \times \left[\sum_i \lambda_i \times C_i(k^*) \right], \quad (3)$$

where the sum contains all femtoscopic contributions $C_i(k^*)$ namely the genuine as well as contamination induced by the misidentification background and feed-down. Each of them is multiplied with its relative contribution λ_i . The $C_{\text{non-femto}}(k^*)$ describes non-femtoscopic effects such as energy conservation which are dominant for large k^* . It is modelled phenomenologically by a polynomial with a constant and a third degree term $C_{\text{non-femto}}(k^*) = a \times (1 - b \times k^3)$, which ensures a flat behaviour at $k^* \rightarrow 0$, and is fitted to the measured correlation function.

In the feed-down contributions, at least one particle of the pair originates from a decay and appears on timescales larger than the strong interaction which is measured here. They carry the residual correlation from their mother particle which is washed out because of the decay. The main feed-down to the Λ ($\bar{\Lambda}$) candidates comes from the Ξ^- (Ξ^+), Ξ^0 (Ξ^0), and Σ^0 (Σ^0) decays. The combined relative contribution is obtained by fitting the CPA distribution to MC templates. Then, the λ parameter for each contribution is determined via isospin considerations. The feed-down to the Ξ^- (Ξ^+) candidates comes from the decays of the resonances $\Xi^-(1530)$ and $\Xi^0(1530)$ as well as the $\Omega^-(\Omega^+)$ hyperons. Their λ parameters are extracted from the production rates reported in Refs. [31,43] and their branching ratios [44]. All feed-down contributions to the correlation function are assumed to be constant in k^* with a value equal to unity, except for the case of the $\Xi^--\Xi^-$ feed-down, with the identified Λ coming from the decay of an unidentified Ξ^- . The latter contributes with $\lambda_{\Xi^--\Xi^-} = 8\%$; it is modelled assuming a pure Coulomb $\Xi^--\Xi^-$ interaction and it is propagated to $C_{\text{model}}(k^*)$ via a momentum transformation from the $\Xi^--\Xi^-$ to the $\Lambda-\Xi^-$ pair rest frame. The relative contribution of all the other feed-down contributions is of $\lambda_{\text{flat}} = 48\%$.

The relative contribution from misidentification is of $\lambda_{\text{mis.}} = 12\%$ and is calculated from the purities in the selection of the Λ and Ξ^- . This contribution is modelled by a second order polynomial $C_{\text{mis.}}(k^*) = p_0 + p_1 k^* + p_2 k^{*2}$ with parameters obtained via a fit to the correlation function constructed using $\Lambda-\Xi^-$ pairs from an invariant mass sideband analysis [45]. The values of the

parameters are $p_0 = 1.22$, $p_1 = -8.94 \times 10^{-4}$ (MeV/c) $^{-1}$, and $p_2 = 8.90 \times 10^{-7}$ (MeV/c) $^{-2}$.

The relative contribution from the genuine Λ - Ξ^- interaction is $\lambda_{\text{genuine}} = 32\%$. In order to consider the finite momentum resolution, evaluated via full simulations of the ALICE apparatus and its response, $C_{\text{model}}(k^*)$ has to be transformed into the basis of the reconstructed momenta as it was done in previous analysis [25].

4. Results

The experimental Λ - Ξ^- correlation function is shown in Fig. 2 in two different k^* and $C(k^*)$ ranges. The systematic uncertainties of the data displayed in Fig. 2 are associated with variations on the selection criteria of Λ ($\bar{\Lambda}$) and Ξ^- ($\bar{\Xi}^+$) as explained in Section 2. The analysis is repeated with 39 random combinations of such variations. For each k^* point, the final systematic uncertainty is given by the width of a Gaussian fit including all 39 measurements of the correlation function.

The data are compared in Fig. 2 with predictions of the correlation function, according to Eq. 3, from several theoretical descriptions of the Λ - Ξ^- strong interaction and from the assumption of no interaction. The parameter of the non-femtoscopic baseline is fitted to the data for each case in the range $k^* \in [0, 800]$ MeV/c. The width of the theoretical bands reflect the uncertainties in the evaluation of the correlation function, namely: i) variations of the radius of the source function according to the experimental determination $r_{\text{eff}} = 1.032^{+0.055}_{-0.056}$ fm; ii) variation of the normalization range by ± 50 MeV/c; iii) variation of the range of the fit to the non-femtoscopic baseline by ± 50 MeV/c; iv) variation in the parametrization of the baseline using a second order polynomial (i.e. the non-femto contribution becomes $C_{\text{non-femto}}(k^*) = a' \times (1 - b' \times k^{*2})$); and v) variation of the functional form describing the sidebands correlation function to $p_0 + \exp(p_1 + p_2 k^*)$. The evaluation of the theoretical correlation function and the fit of the baseline parameters were performed with all possible combinations of such variations. The width of the theoretical band for each model is given in each k^* point by the root mean squared of all fit results.

The dotted black line in Fig. 2 represents the result of the baseline fit assuming no Λ - Ξ^- strong interaction, for which $a = 0.95$ and $b = 2.4 \times 10^{-10}$ (MeV/c) $^{-3}$ are obtained. The compatibility with the data is evaluated in terms of the number of standard deviations n_σ , which were obtained from the p-value computed in the range $k^* < 200$ MeV/c. The uncertainties of the data were considered by adding the statistical and systematic uncertainties in quadrature. The result for the “no strong interaction” assumption is $n_\sigma = 0.78$ showing that in the low relative momentum region, where femtoscopic effects are expected, data do not deviate significantly from the baseline.

The dark blue and light blue bands in the left panel of Fig. 2 represent the correlation function evaluated from LO χ EFT [11] for a regulator function cut-off of 550 and 700 MeV, respectively. The genuine Λ - Ξ^- correlation function is evaluated by using the LL model with the scattering parameters for Λ - Ξ provided in Ref. [11]. The scattering length in this case indicates a rather strong attraction in the singlet channel and a mild repulsion in the triplet channel. The predicted values depend strongly on the cut-off choice, which is reflected in the correlation function. The curve corresponding to the LO χ EFT potential with 550 MeV cut-off, with rather large scattering length, is not compatible with the experimental correlation function. On the other hand, the result for the potential with cut-off 700 MeV is close to the data. However, this interaction implies the presence of a shallow Λ Ξ bound state with a binding energy of just 0.43 MeV. Such bound states are not seen anymore in the extrapolation of the NLO interactions from $S = -2$ [14,15] to $S = -3$ [16], where effects from SU(3)

symmetry breaking have been properly accounted for, in line with the power counting. They are also not supported by the available lattice QCD simulations close to the physical point [2]. The correlation functions expected from the NLO calculations, based on NLO16 [14] and NLO19 [15], are represented by the magenta and green bands in the left panel of Fig. 2, respectively. The dark and light bands represent the interactions with regulator function cut-offs of 500 and 650 MeV, respectively, for both potentials. The correlation function was evaluated by using the LL model with the scattering lengths¹ provided in Ref. [16]. The NLO19 potential is more attractive than the NLO16 in the triplet channel, and there is also a sizable cut-off dependence. This is reflected in a larger correlation function, in particular for the 500 MeV cut-off (dark green band), that clearly exceeds the data. This demonstrates that the ALICE data delivers important constraints in the $S = -3$ sector needed to fix the free parameters in the χ EFT NLO calculations [16].

The Nijmegen meson exchange model [12] predicts the existence of a Σ Ξ bound state, though in the case of the Λ - Ξ^- channel, for 5 of the 6 different versions of the model, a mild attraction and a mild repulsion in the singlet and triplet configurations, respectively, are predicted. The light orange band in Fig. 2 shows the expectation from the version NSC97a. The substantially smaller scattering lengths in the singlet state compared to the χ EFT potentials are reflected in a suppressed correlation function that agrees with the data.

It is worth mentioning that the scattering parameters from the quark constituent model fss2 [13] coincide qualitatively with the Nijmegen potential, although that model does not predict any Σ Ξ or Λ Ξ bound states.

The right panel of Fig. 2 shows the comparison with the results for the HAL QCD Λ - Ξ^- potential [2]. The width of the HAL QCD curves include statistical and systematic variations of the lattice calculations following the recipe in Ref. [7]. The HAL QCD potential is a Λ Ξ - Σ Ξ coupled-channel potential. It presents attraction in both the singlet and the triplet configurations but does not predict the formation of any bound state. The orange curve shows the results from an effective Λ - Ξ^- potential, where the coupling to Σ - Ξ from the lattice simulations is incorporated effectively into the strength of the Λ - Ξ^- interaction. For reference, the red curve shows the correlation function from the Λ Ξ - Λ Ξ elastic potential alone, free of effects from the coupling. The difference between the orange and red curves in Figs. 2 and 1 demonstrates a rather strong coupling. This is particularly noticeable if the results are compared to the HAL QCD p Ξ - Λ Λ potential in the $|S| = 2$ sector [1], in which case the coupling between channels is small and has negligible effects in the correlation function [46]. While the ALICE data shows better compatibility with the single channel Λ Ξ - Λ Ξ elastic potential, it is not sensitive to the effects of the coupling as shown by Lattice QCD.

Threshold cusp-like structures at the channel opening created by the inelastic channels could be formed [47] with an amplitude depending on the properties of the interaction, the strength of the coupling between channels, and the amount of initial state pairs in the inelastic channels. The ALICE data do not present significant structures at the kinematic opening of the Σ^- - Ξ^0 , Σ^0 - Ξ^- and n - Ω^- channels, at k^* values of 303, 308 and 468 MeV/c respectively.

The scattering parameters of all considered interactions are summarized in Table 1, together with the compatibility of each of them with the Λ - Ξ^- correlation function in terms of n_σ computed in the range $k^* < 200$ MeV/c, considering the statistical and

¹ For the triplet state in NLO16 the effective range is set to $d_0 = 0$ fm. This is necessary since the LL does not provide stable results for the large effective ranges predicted by the theory (see Table 1) in combination with the small source radius.

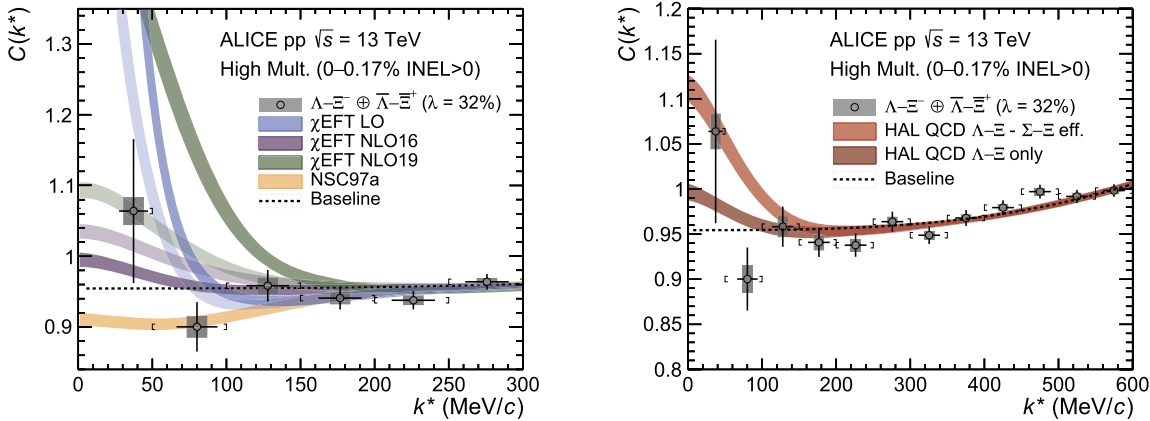


Fig. 2. Experimental $\Lambda-\Xi^-$ correlation function with statistical (vertical black lines) and systematic (gray boxes) uncertainties. The square brackets show the bin width of the measurement and the horizontal black lines represent the statistical uncertainty in the determination of the mean k^* for each bin. Left panel: Comparison to LO [11] and NLO [16] χ EFT and NSC97a [12] potentials evaluated with the Lednický-Lyuboshits model [40,41]. In the χ EFT models the darker and light bands correspond to the version with the lower and higher cut-off value, respectively. Right panel: Comparison with Lattice QCD calculations by the HAL QCD Collaboration [2] using an effective potential including the coupling to $\Sigma-\Xi$ (orange) and the $\Lambda-\Xi^-$ elastic potential alone (red). The width of the bands in both panels correspond to the systematic uncertainties of the fit as described in the text. The dotted black line represents the result of the baseline fit assuming no $\Lambda-\Xi^-$ strong interaction.

Table 1

Summary of scattering parameters and agreement with the data in terms of n_σ of the considered interactions. The effective range parameters for the Lattice QCD results are obtained from the low-energy phase shifts which are extracted with CATS in the evaluation of the potentials. The agreement of the baseline (no interaction assumed) is also given.

Potential	Cut-off (MeV) / version	Singlet		Triplet		n_σ
		f_0^0	d_0^0	f_0^1	d_0^1	
χ EFT LO [11]	550	33.5	1.00	-0.33	-0.36	3.06 – 5.12
	700	-9.07	0.87	-0.31	-0.27	0.78 – 1.60
χ EFT NLO16 [14]	500	0.99	5.77	-0.026	142.9	0.56 – 0.93
	650	0.91	4.63	0.12	32.02	0.91 – 1.61
χ EFT NLO19 [15]	500	0.99	5.77	1.66	1.49	5.47 – 7.26
	650	0.91	4.63	0.42	6.33	1.30 – 2.10
NSC97a [12]		0.80	4.71	-0.54	-0.47	0.68 – 1.04
HAL QCD [2]	$\Lambda\Xi-\Sigma\Xi$ eff.	0.60	6.01	0.50	5.36	1.43 – 2.34
	$\Lambda\Xi-\Lambda\Xi$ only	–	–	–	–	0.64 – 1.04
Baseline		–	–	–	–	0.78

systematic uncertainties of the data. The scattering parameters of the HAL QCD calculations were extracted using CATS by fitting the phase shifts δ_0 with the effective range approximation [48,49].

5. Summary

This Letter presents the first measurement of the $\Lambda-\Xi^-$ interaction, quantified via the correlation function $C(k^*)$ in high-multiplicity pp collisions at $\sqrt{s} = 13$ TeV. The measured $C(k^*)$ were compared with different descriptions of the $\Lambda-\Xi^-$ interaction, including leading-order and next-to-leading-order chiral Effective Field Theory calculations, a meson exchange model, and recent Lattice QCD calculations. Despite the limited statistical significance and the contamination from feed-down contributions, the data provide the first constraint for theoretical investigations and are seen to be more compatible with predictions of small scattering parameters and hence a weak $\Lambda-\Xi^-$ interaction. The limitations of the data sample prevent from drawing further conclusions on the influence of coupled channels in the correlation function, and no significant cusp-like structures are observed at the opening of the $\Sigma^-\Xi^0$, $\Sigma^0\Xi^-$ or $n\Omega^-$ channels. The presented data demonstrate that the characteristics of the strong interaction in the $|S| = 3$ sector can be investigated with the femtoscopy technique. New measurements with the upgraded ALICE apparatus [50] will exploit the data collected during upcoming LHC Run 3 and Run 4 [51,52] and should deliver a precise insight into the $\Lambda-\Xi^-$ interaction, providing valuable information for the search of di-baryon states with strangeness content.

Declaration of competing interest

The authors declare that they have no known competing financial interests or personal relationships that could have appeared to influence the work reported in this paper.

Acknowledgements

The ALICE Collaboration would like to thank all its engineers and technicians for their invaluable contributions to the construction of the experiment and the CERN accelerator teams for the outstanding performance of the LHC complex. The ALICE Collaboration gratefully acknowledges the resources and support provided by all Grid centres and the Worldwide LHC Computing Grid (WLCG) collaboration. The ALICE Collaboration acknowledges the following funding agencies for their support in building and running the ALICE detector: A. I. Alikhanyan National Science Laboratory (Yerevan Physics Institute) Foundation (ANSL), State Committee of Science and World Federation of Scientists (WFS), Armenia; Austrian Academy of Sciences, Austrian Science Fund (FWF): [M 2467-N36] and Nationalstiftung für Forschung, Technologie und Entwicklung, Austria; Ministry of Communications and High Technologies, National Nuclear Research Center, Azerbaijan; Conselho Nacional de Desenvolvimento Científico e Tecnológico (CNPq), Financiadora de Estudos e Projetos (Finep), Fundação de Amparo à Pesquisa do Estado de São Paulo (FAPESP) and Universidade Federal do Rio Grande do Sul (UFRGS), Brazil; Bulgarian Ministry of Education and Science, within the National Roadmap for Re-

search Infrastructures 2020–2027 (object CERN), Bulgaria; Ministry of Education of China (MOEC), Ministry of Science & Technology of China (MSTC) and National Natural Science Foundation of China (NSFC), China; Ministry of Science and Education and Croatian Science Foundation, Croatia; Centro de Aplicaciones Tecnológicas y Desarrollo Nuclear (CEADEN), Cubaenergía, Cuba; Ministry of Education, Youth and Sports of the Czech Republic, Czech Republic; The Danish Council for Independent Research | Natural Sciences, the Villum Fonden and Danish National Research Foundation (DNRF), Denmark; Helsinki Institute of Physics (HIP), Finland; Commissariat à l'Énergie Atomique Atomique (CEA) and Institut National de Physique Nucléaire et de Physique des Particules (IN2P3) and Centre National de la Recherche Scientifique (CNRS), France; Bundesministerium für Bildung und Forschung (BMBF) and GSI Helmholtzzentrum für Schwerionenforschung GmbH, Germany; General Secretariat for Research and Technology, Ministry of Education, Research and Religions, Greece; National Research, Development and Innovation Office, Hungary; Department of Atomic Energy, Government of India (DAE), Department of Science and Technology, Government of India (DST), University Grants Commission, Government of India (UGC) and Council of Scientific and Industrial Research (CSIR), India; National Research and Innovation Agency - BRIN, Indonesia; Istituto Nazionale di Fisica Nucleare (INFN), Italy; Japanese Ministry of Education, Culture, Sports, Science and Technology (MEXT) and Japan Society for the Promotion of Science (JSPS) KAKENHI, Japan; Consejo Nacional de Ciencia y Tecnología (CONACYT), through Fondo de Cooperación Internacional en Ciencia y Tecnología (FONCICYT) and Dirección General de Asuntos del Personal Académico (DGAPA), Mexico; Nederlandse Organisatie voor Wetenschappelijk Onderzoek (NWO), Netherlands; The Research Council of Norway, Norway; Commission on Science and Technology for Sustainable Development in the South (COMSATS), Pakistan; Pontificia Universidad Católica del Perú, Peru; Ministry of Education and Science, National Science Centre and WUT ID-UB, Poland; Korea Institute of Science and Technology Information and National Research Foundation of Korea (NRF), Republic of Korea; Ministry of Education and Scientific Research, Institute of Atomic Physics, Ministry of Research and Innovation and Institute of Atomic Physics and University Politehnica of Bucharest, Romania; Ministry of Education, Science, Research and Sport of the Slovak Republic, Slovakia; National Research Foundation of South Africa, South Africa; Swedish Research Council (VR) and Knut & Alice Wallenberg Foundation (KAW), Sweden; European Organization for Nuclear Research, Switzerland; Suranaree University of Technology (SUT), National Science and Technology Development Agency (NSTDA), Thailand Science Research and Innovation (TSRI) and National Science, Research and Innovation Fund (NSRF), Thailand; Turkish Energy, Nuclear and Mineral Research Agency (TEN-MAK), Turkey; National Academy of Sciences of Ukraine, Ukraine; Science and Technology Facilities Council (STFC), United Kingdom; National Science Foundation of the United States of America (NSF) and United States Department of Energy, Office of Nuclear Physics (DOE NP), United States of America. In addition, individual groups or members have received support from: Marie Skłodowska Curie, Strong 2020 - Horizon 2020, European Research Council (grant nos. 824093, 896850, 950692), European Union; Academy of Finland (Center of Excellence in Quark Matter) (grant nos. 346327, 346328), Finland; Programa de Apoyos para la Superación del Personal Académico, UNAM, Mexico.

References

- [1] K. Sasaki, et al., $\Lambda\Lambda$ and $N\Xi$ interactions from Lattice QCD near the physical point, *Nucl. Phys. A* 998 (2020) 121737.
- [2] N. Ishii, et al., Baryon interactions from lattice QCD with physical masses $-S = -3$ sector: $\Xi\Sigma$ and $\Xi\Sigma-\Lambda\Sigma-$, *EPJ Web Conf.* 175 (2018) 05013.
- [3] HAL QCD Collaboration, T. Iritani, et al., $N\Omega$ dibaryon from lattice QCD near the physical point, *Phys. Lett. B* 792 (2019) 284–289, arXiv:1810.03416 [hep-lat].
- [4] S. Gongyo, et al., Most strange dibaryon from Lattice QCD, *Phys. Rev. Lett.* 120 (21) (2018) 212001, arXiv:1709.00654 [hep-lat].
- [5] T. Sekihara, Y. Kamiya, T. Hyodo, $N\Omega$ interaction: meson exchanges, inelastic channels, and quasibound state, *Phys. Rev. C* 98 (1) (2018) 015205, arXiv:1805.04024 [hep-ph].
- [6] STAR Collaboration, J. Adam, et al., The proton- Ω correlation function in $Au + Au$ collisions at $\sqrt{s_{NN}} = 200$ GeV, *Phys. Lett. B* 790 (2019) 490–497, arXiv: 1808.02511 [hep-ex].
- [7] ALICE Collaboration, S. Acharya, et al., Unveiling the strong interaction among hadrons at the LHC, *Nature* 588 (2020) 232–238, arXiv:2005.11495 [nucl-ex].
- [8] Y. Kamiya, T. Hyodo, K. Morita, A. Ohnishi, W. Weise, K^-p correlation function from high-energy nuclear collisions and chiral SU(3) dynamics, *Phys. Rev. Lett.* 124 (13) (2020) 132501, arXiv:1911.01041 [nucl-th].
- [9] K. Morita, A. Ohnishi, F. Etmiran, T. Hatsuda, Probing multistrange dibaryons with proton-omega correlations in high-energy heavy ion collisions, *Phys. Rev. C* 94 (3) (2016) 031901, arXiv:1605.06765 [hep-ph]; Erratum: *Phys. Rev. C* 100 (2019) 069902.
- [10] K. Morita, S. Gongyo, T. Hatsuda, T. Hyodo, Y. Kamiya, A. Ohnishi, Probing $\Omega\Omega$ and $p\Omega$ dibaryons with femtoscopic correlations in relativistic heavy-ion collisions, *Phys. Rev. C* 101 (2020) 015201, arXiv:1908.05414 [nucl-th].
- [11] J. Haidenbauer, U.-G. Meißner, Predictions for the strangeness $S = -3$ and -4 baryon-baryon interactions in chiral effective field theory, *Phys. Lett. B* 684 (2010) 275–280, arXiv:0907.1395 [nucl-th].
- [12] V.G.J. Stoks, T.A. Rijken, Soft core baryon baryon potentials for the complete baryon octet, *Phys. Rev. C* 59 (1999) 3009–3020, arXiv:nucl-th/9901028.
- [13] Y. Fujiwara, Y. Suzuki, C. Nakamoto, Baryon-baryon interactions in the SU(6) quark model and their applications to light nuclear systems, *Prog. Part. Nucl. Phys.* 58 (2007) 439–520, arXiv:nucl-th/0607013.
- [14] J. Haidenbauer, U.-G. Meißner, S. Petschauer, Strangeness $S = -2$ baryon-baryon interaction at next-to-leading order in chiral effective field theory, *Nucl. Phys. A* 954 (2016) 273–293, arXiv:1511.05859 [nucl-th].
- [15] J. Haidenbauer, U.-G. Meißner, In-medium properties of a ΞN interaction derived from chiral effective field theory, *Eur. Phys. J. A* 55 (2) (2019) 23, arXiv: 1810.04883 [nucl-th].
- [16] J. Haidenbauer, U.-G. Meißner, Strangeness $S = -3$ and -4 baryon-baryon interactions in chiral effective field theory, in: 10th International Workshop on Chiral Dynamics, 1, 2022, arXiv:2201.08238 [nucl-th].
- [17] M. Danysz, et al., The identification of a double hyperfragment, *Nucl. Phys.* 49 (1963) 121–132.
- [18] H. Takahashi, et al., Observation of a $^6_{\Lambda\Lambda}$ He double hypernucleus, *Phys. Rev. Lett.* 87 (2001) 212502.
- [19] KEK E176 Collaboration, S. Aoki, et al., Nuclear capture at rest of Ξ^- hyperons, *Nucl. Phys. A* 828 (2009) 191–232.
- [20] E373 (KEK-PS) Collaboration, J.K. Ahn, et al., Double- Λ hypernuclei observed in a hybrid emulsion experiment, *Phys. Rev. C* 88 (1) (2013) 014003.
- [21] K. Nakazawa, et al., The first evidence of a deeply bound state of $\Xi^-{}^{14}N$ system, *PTEP* 2015 (2015) 033D02.
- [22] J-PARC E07 Collaboration, S.H. Hayakawa, et al., Observation of Coulomb-assisted nuclear bound state of $\Xi^-{}^{14}N$ system, *Phys. Rev. Lett.* 126 (6) (2021) 062501, arXiv:2010.14317 [nucl-ex].
- [23] L. Fabbietti, V.M. Sarti, O.V. Doce, Study of the strong interaction among hadrons with correlations at the LHC, *Annu. Rev. Nucl. Part. Sci.* 71 (2021) 377–402, arXiv:2012.09806 [nucl-ex].
- [24] STAR Collaboration, L. Adamczyk, et al., $\Lambda\Lambda$ correlation function in $Au+Au$ collisions at $\sqrt{s_{NN}} = 200$ GeV, *Phys. Rev. Lett.* 114 (2015) 022301, arXiv:1408.4360 [nucl-ex].
- [25] ALICE Collaboration, S. Acharya, et al., p-p, p- Λ and Λ - Λ correlations studied via femtoscopy in pp reactions at $\sqrt{s} = 7$ TeV, *Phys. Rev. C* 99 (2019) 024001, arXiv:1805.12455 [nucl-ex].
- [26] ALICE Collaboration, S. Acharya, et al., Study of the Λ - Λ interaction with femtoscopy correlations in pp and p-Pb collisions at the LHC, *Phys. Lett. B* 797 (2019) 134822, arXiv:1905.07209 [nucl-ex].
- [27] ALICE Collaboration, S. Acharya, et al., First observation of an attractive interaction between a proton and a cascade baryon, *Phys. Rev. Lett.* 123 (2019) 112002, arXiv:1904.12198 [nucl-ex].
- [28] ALICE Collaboration, K. Aamodt, et al., The ALICE experiment at the CERN LHC, *J. Instrum.* 3 (2008) S08002.
- [29] ALICE Collaboration, B. Abelev, et al., Performance of the ALICE experiment at the CERN LHC, *Int. J. Mod. Phys. A* 29 (2014) 1430044.
- [30] ALICE Collaboration, E. Abbas, et al., Performance of the ALICE VZERO system, *J. Instrum.* 8 (2013) P10016, arXiv:1306.3130 [nucl-ex].
- [31] ALICE Collaboration, J. Adam, et al., Enhanced production of multi-strange hadrons in high-multiplicity proton-proton collisions, *Nat. Phys.* 13 (2017) 535–539, arXiv:1606.07424 [nucl-ex].
- [32] ALICE Collaboration, K. Aamodt, et al., Alignment of the ALICE inner tracking system with cosmic-ray tracks, *J. Instrum.* 5 (2010) P03003, arXiv:1001.0502 [physics.ins-det].

- [33] J. Alme, et al., The ALICE TPC, a large 3-dimensional tracking device with fast readout for ultra-high multiplicity events, Nucl. Instrum. Methods A 622 (2010) 316–367, arXiv:1001.1950 [physics.ins-det].
- [34] A. Akindinov, et al., Performance of the ALICE time-of-flight detector at the LHC, Eur. Phys. J. Plus 128 (2013) 44.
- [35] ALICE Collaboration, K. Aamodt, et al., Strange particle production in proton-proton collisions at $\sqrt{s} = 0.9$ TeV with ALICE at the LHC, Eur. Phys. J. C 71 (2011) 1594, arXiv:1012.3257 [hep-ex].
- [36] T. Sjöstrand, S. Ask, J.R. Christiansen, R. Corke, N. Desai, P. Ilten, S. Mrenna, S. Prestel, C.O. Rasmussen, P.Z. Skands, An introduction to PYTHIA 8.2, Comput. Phys. Commun. 191 (2015) 159–177, arXiv:1410.3012 [hep-ph].
- [37] R. Brun, R. Hagelberg, M. Hansroul, J.C. Lassalle, Simulation Program for Particle Physics Experiments, GEANT: User Guide and Reference Manual, CERN, Geneva, 1978, <https://cds.cern.ch/record/118715>.
- [38] M.A. Lisa, S. Pratt, R. Soltz, U. Wiedemann, Femtoscopy in relativistic heavy ion collisions: two decades of progress, Annu. Rev. Nucl. Part. Sci. 55 (2005) 357–402, arXiv:nucl-ex/0505014 [nucl-ex].
- [39] ALICE Collaboration, S. Acharya, et al., Search for a common baryon source in high-multiplicity pp collisions at the LHC, Phys. Lett. B 811 (2020) 135849, arXiv:2004.08018 [nucl-ex].
- [40] R. Lednický, V. Lyuboshits, Final state interaction effect on pairing correlations between particles with small relative momenta, Sov. J. Nucl. Phys. 35 (1982) 770.
- [41] A. Stavinskiy, K. Mikhailov, B. Erazmus, R. Lednický, Residual correlations between decay products of $\pi^0\pi^0$ and $p\Sigma^0$ systems, arXiv:0704.3290 [nucl-th].
- [42] D. Mihaylov, V. Mantovani Sarti, O. Arnold, L. Fabbietti, B. Hohlweier, A. Mathis, A femtosopic correlation analysis tool using the Schrödinger equation (CATS), Eur. Phys. J. C 78 (2018) 394, arXiv:1802.08481 [hep-ph].
- [43] ALICE Collaboration, B. Abelev, et al., Production of $\Sigma(1385)^{\pm}$ and Ξ^0 (1530) in proton-proton collisions at $\sqrt{s} = 7$ TeV, Eur. Phys. J. C 75 (2015) 1, arXiv: 1406.3206 [nucl-th].
- [44] Particle Data Group Collaboration, P.A. Zyla, et al., Review of particle physics, Prog. Theor. Exp. Phys. 2020 (8) (2020).
- [45] ALICE Collaboration, S. Acharya, et al., Investigation of the p- Σ^0 interaction via femtoscopy in pp collisions, Phys. Lett. B 805 (2020) 135419, arXiv:1910.14407 [nucl-ex].
- [46] Y. Kamiya, K. Sasaki, T. Fukui, T. Hyodo, K. Morita, K. Ogata, A. Ohnishi, T. Hatsuda, Femtoscopic study of coupled-channel $N\Xi$ and $\Lambda\Lambda$ interactions, YITP-21-79, RIKEN-iTHEMS-Report-21, NITEP 116, arXiv:2108.09644 [hep-ph].
- [47] J. Haidenbauer, Coupled-channel effects in hadron-hadron correlation functions, Nucl. Phys. A 981 (2019) 1–16, arXiv:1808.05049 [hep-ph].
- [48] J.J. Sakurai, J. Napolitano, Modern Quantum Mechanics, 2nd ed., Cambridge University Press, 2017, pp. 388–400.
- [49] D. Griffiths, Introduction to Quantum Mechanics, Pearson international edition, Pearson Prentice Hall, 2005, pp. 394–407.
- [50] ALICE Collaboration, B. Abelev, et al., Upgrade of the ALICE experiment: letter of intent, J. Phys. G 41 (2014) 087001.
- [51] Z. Citron, et al., Report from working group 5: future physics opportunities for high-density QCD at the LHC with heavy-ion and proton beams, CERN Yellow Rep. Monogr. 7 (2019) 1159–1410.
- [52] ALICE Collaboration, S. Acharya, et al., Future high-energy pp programme with ALICE, ALICE-PUBLIC-2020-005, CERN-LHCC-2020-018, <https://cds.cern.ch/record/2724925>.

ALICE Collaboration

- S. Acharya ^{127, 134,} , D. Adamová ^{87,} , A. Adler ⁷⁰, G. Aglieri Rinella ^{32,} , M. Agnello ^{29,} , N. Agrawal ^{50,} , Z. Ahammed ^{134,} , S. Ahmad ^{15,} , S.U. Ahn ^{71,} , I. Ahuja ^{37,} , A. Akindinov ^{142,} , M. Al-Turany ^{100,} , D. Aleksandrov ^{142,} , B. Alessandro ^{55,} , H.M. Alfanda ^{6,} , R. Alfaro Molina ^{67,} , B. Ali ^{15,} , Y. Ali ¹³, A. Alici ^{25,} , N. Alizadehvandchali ^{116,} , A. Alkin ^{32,} , J. Alme ^{20,} , G. Alocco ^{51,} , T. Alt ^{64,} , I. Altsybeev ^{142,} , M.N. Anaam ^{6,} , C. Andrei ^{45,} , A. Andronic ^{137,} , V. Anguelov ^{96,} , F. Antinori ^{53,} , P. Antonioli ^{50,} , C. Anuj ^{15,} , N. Apadula ^{75,} , L. Aphecetche ^{106,} , H. Appelshäuser ^{64,} , S. Arcelli ^{25,} , R. Arnaldi ^{55,} , I.C. Arsene ^{19,} , M. Arslanbekov ^{139,} , A. Augustinus ^{32,} , R. Averbeck ^{100,} , S. Aziz ^{73,} , M.D. Azmi ^{15,} , A. Badalà ^{52,} , Y.W. Baek ^{40,} , X. Bai ^{100,} , R. Bailhache ^{64,} , Y. Bailung ^{47,} , R. Bala ^{92,} , A. Balbino ^{29,} , A. Baldissari ^{130,} , B. Balis ^{2,} , D. Banerjee ^{4,} , Z. Banoo ^{92,} , R. Barbera ^{26,} , L. Barioglio ^{97,} , M. Barlou ⁷⁹, G.G. Barnaföldi ^{138,} , L.S. Barnby ^{86,} , V. Barret ^{127,} , L. Barreto ^{112,} , C. Bartels ^{119,} , K. Barth ^{32,} , E. Bartsch ^{64,} , F. Baruffaldi ^{27,} , N. Bastid ^{127,} , S. Basu ^{76,} , G. Batigne ^{106,} , D. Battistini ^{97,} , B. Batyunya ^{143,} , D. Bauri ⁴⁶, J.L. Bazo Alba ^{104,} , I.G. Bearden ^{84,} , C. Beattie ^{139,} , P. Becht ^{100,} , D. Behera ^{47,} , I. Belikov ^{129,} , A.D.C. Bell Hechavarria ^{137,} , F. Bellini ^{25,} , R. Bellwied ^{116,} , S. Belokurova ^{142,} , V. Belyaev ^{142,} , G. Bencedi ^{138, 65,} , S. Beole ^{24,} , A. Bercuci ^{45,} , Y. Berdnikov ^{142,} , A. Berdnikova ^{96,} , L. Bergmann ^{96,} , M.G. Besoiu ^{63,} , L. Betev ^{32,} , P.P. Bhaduri ^{134,} , A. Bhasin ^{92,} , I.R. Bhat ⁹², M.A. Bhat ^{4,} , B. Bhattacharjee ^{41,} , L. Bianchi ^{24,} , N. Bianchi ^{48,} , J. Bielčík ^{35,} , J. Bielčíková ^{87,} , J. Biernat ^{109,} , A. Bilandzic ^{97,} , G. Biro ^{138,} , S. Biswas ^{4,} , J.T. Blair ^{110,} , D. Blau ^{142,} , M.B. Blidaru ^{100,} , N. Bluhme ³⁸, C. Blume ^{64,} , G. Boca ^{21, 54,} , F. Bock ^{88,} , T. Bodova ^{20,} , A. Bogdanov ¹⁴², S. Boi ^{22,} , J. Bok ^{57,} , L. Boldizsár ^{138,} , A. Bolozdynya ^{142,} , M. Bombara ^{37,} , P.M. Bond ^{32,} , G. Bonomi ^{133, 54,} , H. Borel ^{130,} , A. Borissov ^{142,} , H. Bossi ^{139,} , E. Botta ^{24,} , L. Bratrud ^{64,} , P. Braun-Munzinger ^{100,} , M. Bregant ^{112,} , M. Broz ^{35,} , G.E. Bruno ^{98, 31,} , M.D. Buckland ^{119,} , D. Budnikov ^{142,} , H. Buesching ^{64,} , S. Bufalino ^{29,} , O. Bugnon ¹⁰⁶, P. Buhler ^{105,} , Z. Buthelezi ^{68, 123,} , J.B. Butt ¹³, A. Bylinkin ^{118,} , S.A. Bysiak ¹⁰⁹, M. Cai ^{27, 6,} , H. Caines ^{139,} , A. Caliva ^{100,} , E. Calvo Villar ^{104,} ,

- J.M.M. Camacho 111, ID, R.S. Camacho 44, P. Camerini 23, ID, F.D.M. Canedo 112, ID, M. Carabas 126, ID,
 F. Carnesecchi 32, ID, R. Caron 128, 130, ID, J. Castillo Castellanos 130, ID, F. Catalano 29, ID, C. Ceballos
 Sanchez 143, ID, I. Chakaberia 75, ID, P. Chakraborty 46, ID, S. Chandra 134, ID, S. Chapeland 32, ID,
 M. Chartier 119, ID, S. Chattopadhyay 134, ID, S. Chattopadhyay 102, ID, T.G. Chavez 44, ID, T. Cheng 6, ID,
 C. Cheshkov 128, ID, B. Cheynis 128, ID, V. Chibante Barroso 32, ID, D.D. Chinellato 113, ID, E.S. Chizzali 97, ID, II,
 J. Cho 57, ID, S. Cho 57, ID, P. Chochula 32, ID, P. Christakoglou 85, ID, C.H. Christensen 84, ID,
 P. Christiansen 76, ID, T. Chujo 125, ID, M. Ciacco 29, ID, C. Cicalo 51, ID, L. Cifarelli 25, ID, F. Cindolo 50, ID,
 M.R. Ciupek 100, G. Clai 50, III, F. Colamaria 49, ID, J.S. Colburn 103, D. Colella 98, 31, ID, A. Collu 75,
 M. Colocci 32, ID, M. Concas 55, ID, IV, G. Conesa Balbastre 74, ID, Z. Conesa del Valle 73, ID, G. Contin 23, ID,
 J.G. Contreras 35, ID, M.L. Coquet 130, ID, T.M. Cormier 88, I, P. Cortese 132, 55, ID, M.R. Cosentino 114, ID,
 F. Costa 32, ID, S. Costanza 21, 54, ID, P. Crochet 127, ID, R. Cruz-Torres 75, ID, E. Cuautle 65, P. Cui 6, ID,
 L. Cunqueiro 88, A. Dainese 53, ID, M.C. Danisch 96, ID, A. Danu 63, ID, P. Das 81, ID, P. Das 4, ID, S. Das 4, ID,
 S. Dash 46, ID, R.M.H. David 44, A. De Caro 28, ID, G. de Cataldo 49, ID, L. De Cilladi 24, ID, J. de Cuveland 38,
 A. De Falco 22, ID, D. De Gruttola 28, ID, N. De Marco 55, ID, C. De Martin 23, ID, S. De Pasquale 28, ID,
 S. Deb 47, ID, H.F. Degenhardt 112, K.R. Deja 135, R. Del Grande 97, ID, L. Dello Stritto 28, ID, W. Deng 6, ID,
 P. Dhankher 18, ID, D. Di Bari 31, ID, A. Di Mauro 32, ID, R.A. Diaz 143, 7, ID, T. Dietel 115, ID, Y. Ding 128, 6, ID,
 R. Divià 32, ID, D.U. Dixit 18, ID, Ø. Djupsland 20, U. Dmitrieva 142, ID, A. Dobrin 63, ID, B. Dönigus 64, ID,
 A.K. Dubey 134, ID, J.M. Dubinski 135, ID, A. Dubla 100, ID, S. Dudi 91, ID, P. Dupieux 127, ID, M. Durkac 108,
 N. Dzalaiova 12, T.M. Eder 137, ID, R.J. Ehlers 88, ID, V.N. Eikeland 20, F. Eisenhut 64, ID, D. Elia 49, ID,
 B. Erazmus 106, ID, F. Ercolessi 25, ID, F. Erhardt 90, ID, M.R. Ersdal 20, B. Espagnon 73, ID, G. Eulisse 32, ID,
 D. Evans 103, ID, S. Evdokimov 142, ID, L. Fabbietti 97, ID, M. Faggin 27, ID, J. Faivre 74, ID, F. Fan 6, ID, W. Fan 75, ID,
 A. Fantoni 48, ID, M. Fasel 88, ID, P. Fecchio 29, A. Feliciello 55, ID, G. Feofilov 142, ID, A. Fernández Téllez 44, ID,
 M.B. Ferrer 32, ID, A. Ferrero 130, ID, A. Ferretti 24, ID, V.J.G. Feuillard 96, ID, J. Figiel 109, ID, V. Filova 35, ID,
 D. Finogeev 142, ID, F.M. Fionda 51, ID, G. Fiorenza 98, F. Flor 116, ID, A.N. Flores 110, ID, S. Foertsch 68, ID,
 I. Fokin 96, ID, S. Fokin 142, ID, E. Fragiacomo 56, ID, E. Frajna 138, ID, U. Fuchs 32, ID, N. Funicello 28, ID,
 C. Furget 74, ID, A. Furs 142, ID, J.J. Gaardhøje 84, ID, M. Gagliardi 24, ID, A.M. Gago 104, ID, A. Gal 129,
 C.D. Galvan 111, ID, P. Ganoti 79, ID, C. Garabatos 100, ID, J.R.A. Garcia 44, ID, E. Garcia-Solis 9, ID, K. Garg 106, ID,
 C. Gargiulo 32, ID, A. Garibli 82, K. Garner 137, E.F. Gauger 110, ID, A. Gautam 118, ID, M.B. Gay Ducati 66, ID,
 M. Germain 106, ID, S.K. Ghosh 4, M. Giacalone 25, ID, P. Gianotti 48, ID, P. Giubellino 100, 55, ID,
 P. Giubilato 27, ID, A.M.C. Glaenzer 130, ID, P. Glässel 96, ID, E. Glimos 122, ID, D.J.Q. Goh 77, V. Gonzalez 136, ID,
 L.H. González-Trueba 67, ID, S. Gorbunov 38, M. Gorgon 2, ID, L. Görlich 109, ID, S. Gotovac 33, V. Grabski 67, ID,
 L.K. Graczykowski 135, ID, E. Grecka 87, ID, L. Greiner 75, ID, A. Grelli 59, ID, C. Grigoras 32, ID, V. Grigoriev 142, ID,
 S. Grigoryan 143, 1, ID, F. Grossa 32, ID, J.F. Grosse-Oetringhaus 32, ID, R. Grossi 100, ID, D. Grund 35, ID,
 G.G. Guardiano 113, ID, R. Guernane 74, ID, M. Guilbaud 106, ID, K. Gulbrandsen 84, ID, T. Gunji 124, ID,
 W. Guo 6, ID, A. Gupta 92, ID, R. Gupta 92, ID, S.P. Guzman 44, ID, L. Gyulai 138, ID, M.K. Habib 100,
 C. Hadjidakis 73, ID, J. Haidenbauer 58, ID, H. Hamagaki 77, ID, M. Hamid 6, Y. Han 140, ID, R. Hannigan 110, ID,
 M.R. Haque 135, ID, A. Harlenderova 100, J.W. Harris 139, ID, A. Harton 9, ID, J.A. Hasenbichler 32,
 H. Hassan 88, ID, T. Hatsuda 101, ID, D. Hatzifotiadou 50, ID, P. Hauer 42, ID, L.B. Havener 139, ID, S.T. Heckel 97, ID,
 E. Hellbär 100, ID, H. Helstrup 34, ID, T. Herman 35, ID, G. Herrera Corral 8, ID, F. Herrmann 137,
 K.F. Hetland 34, ID, B. Heybeck 64, ID, H. Hillemanns 32, ID, C. Hills 119, ID, B. Hippolyte 129, ID, B. Hofman 59, ID,
 B. Hohlweger 85, ID, J. Honermann 137, ID, G.H. Hong 140, ID, D. Horak 35, ID, A. Horzyk 2, ID, R. Hosokawa 14,
 Y. Hou 6, ID, P. Hristov 32, ID, C. Hughes 122, ID, P. Huhn 64, L.M. Huhta 117, ID, C.V. Hulse 73, ID,

- T.J. Humanic ^{89, ID}, H. Hushnud ¹⁰², A. Hutson ^{116, ID}, D. Hutter ^{38, ID}, J.P. Iddon ^{119, ID}, R. Ilkaev ¹⁴²,
 H. Ilyas ^{13, ID}, M. Inaba ^{125, ID}, G.M. Innocenti ^{32, ID}, M. Ippolitov ^{142, ID}, A. Isakov ^{87, ID}, N. Ishii ⁹⁹,
 T. Isidori ^{118, ID}, M.S. Islam ^{102, ID}, M. Ivanov ^{100, ID}, V. Ivanov ^{142, ID}, V. Izucheev ¹⁴², M. Jablonski ^{2, ID},
 B. Jacak ^{75, ID}, N. Jacazio ^{32, ID}, P.M. Jacobs ^{75, ID}, S. Jadlovska ¹⁰⁸, J. Jadlovsky ¹⁰⁸, L. Jaffe ³⁸, C. Jahnke ^{113, ID},
 M.A. Janik ^{135, ID}, T. Janson ⁷⁰, M. Jercic ⁹⁰, O. Jevons ¹⁰³, A.A.P. Jimenez ^{65, ID}, F. Jonas ^{88,137, ID},
 P.G. Jones ¹⁰³, J.M. Jowett ^{32,100, ID}, J. Jung ^{64, ID}, M. Jung ^{64, ID}, A. Junique ^{32, ID}, A. Jusko ^{103, ID},
 M.J. Kabus ^{32,135, ID}, J. Kaewjai ¹⁰⁷, P. Kalinak ^{60, ID}, A.S. Kalteyer ^{100, ID}, A. Kalweit ^{32, ID}, V. Kaplin ^{142, ID},
 A. Karasu Uysal ^{72, ID}, D. Karatovic ^{90, ID}, O. Karavichev ^{142, ID}, T. Karavicheva ^{142, ID}, P. Karczmarczyk ^{135, ID},
 E. Karpechev ^{142, ID}, V. Kashyap ⁸¹, A. Kazantsev ¹⁴², U. Kebschull ^{70, ID}, R. Keidel ^{141, ID}, D.L.D. Keijdener ⁵⁹,
 M. Keil ^{32, ID}, B. Ketzer ^{42, ID}, A.M. Khan ^{6, ID}, S. Khan ^{15, ID}, A. Khanzadeev ^{142, ID}, Y. Kharlov ^{142, ID},
 A. Khatun ^{15, ID}, A. Khuntia ^{109, ID}, B. Kileng ^{34, ID}, B. Kim ^{16, ID}, C. Kim ^{16, ID}, D.J. Kim ^{117, ID}, E.J. Kim ^{69, ID},
 J. Kim ^{140, ID}, J.S. Kim ^{40, ID}, J. Kim ^{96, ID}, J. Kim ^{69, ID}, M. Kim ^{96, ID}, S. Kim ^{17, ID}, T. Kim ^{140, ID}, S. Kirsch ^{64, ID},
 I. Kisel ^{38, ID}, S. Kiselev ^{142, ID}, A. Kisiel ^{135, ID}, J.P. Kitowski ^{2, ID}, J.L. Klay ^{5, ID}, J. Klein ^{32, ID}, S. Klein ^{75, ID},
 C. Klein-Bösing ^{137, ID}, M. Kleiner ^{64, ID}, T. Klemenz ^{97, ID}, A. Kluge ^{32, ID}, A.G. Knospe ^{116, ID}, C. Kobdaj ^{107, ID},
 T. Kollegger ¹⁰⁰, A. Kondratyev ^{143, ID}, N. Kondratyeva ^{142, ID}, E. Kondratyuk ^{142, ID}, J. Konig ^{64, ID},
 S.A. Konigstorfer ^{97, ID}, P.J. Konopka ^{32, ID}, G. Kornakov ^{135, ID}, S.D. Koryciak ^{2, ID}, A. Kotliarov ^{87, ID},
 O. Kovalenko ^{80, ID}, V. Kovalenko ^{142, ID}, M. Kowalski ^{109, ID}, I. Králik ^{60, ID}, A. Kravčáková ^{37, ID}, L. Kreis ¹⁰⁰,
 M. Krivda ^{103,60, ID}, F. Krizek ^{87, ID}, K. Krizkova Gajdosova ^{35, ID}, M. Kroesen ^{96, ID}, M. Krüger ^{64, ID},
 D.M. Krupova ^{35, ID}, E. Kryshen ^{142, ID}, M. Krzewicki ³⁸, V. Kučera ^{32, ID}, C. Kuhn ^{129, ID}, P.G. Kuijer ^{85, ID},
 T. Kumaoka ¹²⁵, D. Kumar ¹³⁴, L. Kumar ^{91, ID}, N. Kumar ⁹¹, S. Kundu ^{32, ID}, P. Kurashvili ^{80, ID},
 A. Kurepin ^{142, ID}, A.B. Kurepin ^{142, ID}, S. Kushpil ^{87, ID}, J. Kvapil ^{103, ID}, M.J. Kweon ^{57, ID}, J.Y. Kwon ^{57, ID},
 Y. Kwon ^{140, ID}, S.L. La Pointe ^{38, ID}, P. La Rocca ^{26, ID}, Y.S. Lai ⁷⁵, A. Lakrathok ¹⁰⁷, M. Lamanna ^{32, ID},
 R. Langoy ^{121, ID}, P. Larionov ^{48, ID}, E. Laudi ^{32, ID}, L. Lautner ^{32,97, ID}, R. Lavicka ^{105, ID}, T. Lazareva ^{142, ID},
 R. Lea ^{133,54, ID}, J. Lehrbach ^{38, ID}, R.C. Lemmon ^{86, ID}, I. León Monzón ^{111, ID}, M.M. Lesch ^{97, ID},
 E.D. Lesser ^{18, ID}, M. Lettrich ⁹⁷, P. Lévai ^{138, ID}, X. Li ¹⁰, X.L. Li ⁶, J. Lien ^{121, ID}, R. Lietava ^{103, ID}, B. Lim ^{16, ID},
 S.H. Lim ^{16, ID}, V. Lindenstruth ^{38, ID}, A. Lindner ⁴⁵, C. Lippmann ^{100, ID}, A. Liu ^{18, ID}, D.H. Liu ^{6, ID}, J. Liu ^{119, ID},
 I.M. Lofnes ^{20, ID}, V. Loginov ¹⁴², C. Loizides ^{88, ID}, P. Loncar ^{33, ID}, J.A. Lopez ^{96, ID}, X. Lopez ^{127, ID}, E. López
 Torres ^{7, ID}, P. Lu ^{100,120, ID}, J.R. Luhder ^{137, ID}, M. Lunardon ^{27, ID}, G. Luparello ^{56, ID}, Y.G. Ma ^{39, ID},
 A. Maevskaya ¹⁴², M. Mager ^{32, ID}, T. Mahmoud ⁴², A. Maire ^{129, ID}, M. Malaev ^{142, ID}, N.M. Malik ^{92, ID},
 Q.W. Malik ¹⁹, S.K. Malik ^{92, ID}, L. Malinina ^{143, ID, VII}, D. Mal'Kevich ^{142, ID}, D. Mallick ^{81, ID}, N. Mallick ^{47, ID},
 G. Mandaglio ^{30,52, ID}, V. Manko ^{142, ID}, F. Manso ^{127, ID}, G. Mantzaridis ^{97, ID}, V. Manzari ^{49, ID}, Y. Mao ^{6, ID},
 G.V. Margagliotti ^{23, ID}, A. Margotti ^{50, ID}, A. Marín ^{100, ID}, C. Markert ^{110, ID}, M. Marquard ⁶⁴, N.A. Martin ⁹⁶,
 P. Martinengo ^{32, ID}, J.L. Martinez ¹¹⁶, M.I. Martínez ^{44, ID}, G. Martínez García ^{106, ID}, S. Masciocchi ^{100, ID},
 M. Masera ^{24, ID}, A. Masoni ^{51, ID}, L. Massacrier ^{73, ID}, A. Mastroserio ^{131,49, ID}, A.M. Mathis ^{97, ID},
 O. Matonoha ^{76, ID}, P.F.T. Matuoka ¹¹², A. Matyja ^{109, ID}, C. Mayer ^{109, ID}, A.L. Mazuecos ^{32, ID},
 F. Mazzaschi ^{24, ID}, M. Mazzilli ^{32, ID}, J.E. Mdhluli ^{123, ID}, A.F. Mechler ⁶⁴, Y. Melikyan ^{142, ID},
 A. Menchaca-Rocha ^{67, ID}, E. Meninno ^{105,28, ID}, A.S. Menon ^{116, ID}, M. Meres ^{12, ID}, S. Mhlanga ^{115,68},
 Y. Miake ¹²⁵, L. Micheletti ^{55, ID}, L.C. Migliorin ¹²⁸, D.L. Mihaylov ^{97, ID}, K. Mikhaylov ^{143,142, ID},
 A.N. Mishra ^{138, ID}, D. Miśkowiec ^{100, ID}, A. Modak ^{4, ID}, A.P. Mohanty ^{59, ID}, B. Mohanty ⁸¹, M. Mohisin
 Khan ^{15, ID, V}, M.A. Molander ^{43, ID}, Z. Moravcova ^{84, ID}, C. Mordasini ^{97, ID}, D.A. Moreira De Godoy ^{137, ID},
 I. Morozov ^{142, ID}, A. Morsch ^{32, ID}, T. Mrnjavac ^{32, ID}, V. Muccifora ^{48, ID}, E. Mudnic ³³, S. Muhuri ^{134, ID},
 J.D. Mulligan ^{75, ID}, A. Mulliri ²², M.G. Munhoz ^{112, ID}, R.H. Munzer ^{64, ID}, H. Murakami ^{124, ID},

- S. Murray ^{115, ID}, L. Musa ^{32, ID}, J. Musinsky ^{60, ID}, J.W. Myrcha ^{135, ID}, B. Naik ^{123, ID}, R. Nair ^{80, ID},
 B.K. Nandi ^{46, ID}, R. Nania ^{50, ID}, E. Nappi ^{49, ID}, A.F. Nassirpour ^{76, ID}, A. Nath ^{96, ID}, C. Nattrass ^{122, ID},
 A. Neagu ¹⁹, A. Negru ¹²⁶, L. Nellen ^{65, ID}, S.V. Nesbo ³⁴, G. Neskovic ^{38, ID}, D. Nesterov ^{142, ID},
 B.S. Nielsen ^{84, ID}, E.G. Nielsen ^{84, ID}, S. Nikolaev ^{142, ID}, S. Nikulin ^{142, ID}, V. Nikulin ^{142, ID}, F. Noferini ^{50, ID},
 S. Noh ^{11, ID}, P. Nomokonov ^{143, ID}, J. Norman ^{119, ID}, N. Novitzky ^{125, ID}, P. Nowakowski ^{135, ID},
 A. Nyanin ^{142, ID}, J. Nystrand ^{20, ID}, M. Ogino ^{77, ID}, A. Ohlson ^{76, ID}, V.A. Okorokov ^{142, ID}, J. Oleniacz ^{135, ID},
 A.C. Oliveira Da Silva ^{122, ID}, M.H. Oliver ^{139, ID}, A. Onnerstad ^{117, ID}, C. Oppedisano ^{55, ID}, A. Ortiz
 Velasquez ^{65, ID}, A. Oskarsson ⁷⁶, J. Otwinowski ^{109, ID}, M. Oya ⁹⁴, K. Oyama ^{77, ID}, Y. Pachmayer ^{96, ID},
 S. Padhan ^{46, ID}, D. Pagano ^{133, 54, ID}, G. Paić ^{65, ID}, A. Palasciano ^{49, ID}, S. Panebianco ^{130, ID}, J. Park ^{57, ID},
 J.E. Parkkila ^{32, 117, ID}, S.P. Pathak ¹¹⁶, R.N. Patra ⁹², B. Paul ^{22, ID}, H. Pei ^{6, ID}, T. Peitzmann ^{59, ID}, X. Peng ^{6, ID},
 L.G. Pereira ^{66, ID}, H. Pereira Da Costa ^{130, ID}, D. Peresunko ^{142, ID}, G.M. Perez ^{7, ID}, S. Perrin ^{130, ID},
 Y. Pestov ¹⁴², V. Petráček ^{35, ID}, V. Petrov ^{142, ID}, M. Petrovici ^{45, ID}, R.P. Pezzi ^{106, 66, ID}, S. Piano ^{56, ID},
 M. Pikna ^{12, ID}, P. Pillot ^{106, ID}, O. Pinazza ^{50, 32, ID}, L. Pinsky ¹¹⁶, C. Pinto ^{97, 26, ID}, S. Pisano ^{48, ID},
 M. Płoskoń ^{75, ID}, M. Planinic ⁹⁰, F. Pliquet ⁶⁴, M.G. Poghosyan ^{88, ID}, S. Politano ^{29, ID}, N. Poljak ^{90, ID},
 A. Pop ^{45, ID}, S. Porteboeuf-Houssais ^{127, ID}, J. Porter ^{75, ID}, V. Pozdniakov ^{143, ID}, S.K. Prasad ^{4, ID},
 S. Prasad ^{47, ID}, R. Preghenella ^{50, ID}, F. Prino ^{55, ID}, C.A. Pruneau ^{136, ID}, I. Pshenichnov ^{142, ID}, M. Puccio ^{32, ID},
 S. Qiu ^{85, ID}, L. Quaglia ^{24, ID}, R.E. Quishpe ¹¹⁶, S. Ragoni ^{103, ID}, A. Rakotozafindrabe ^{130, ID},
 L. Ramello ^{132, 55, ID}, F. Rami ^{129, ID}, S.A.R. Ramirez ^{44, ID}, T.A. Rancien ⁷⁴, R. Raniwala ^{93, ID}, S. Raniwala ⁹³,
 S.S. Räsänen ^{43, ID}, R. Rath ^{47, ID}, I. Ravasenga ^{85, ID}, K.F. Read ^{88, 122, ID}, A.R. Redelbach ^{38, ID},
 K. Redlich ^{80, ID, VI}, A. Rehman ²⁰, P. Reichelt ⁶⁴, F. Reidt ^{32, ID}, H.A. Reme-Ness ^{34, ID}, Z. Rescakova ³⁷,
 K. Reygers ^{96, ID}, A. Riabov ^{142, ID}, V. Riabov ^{142, ID}, R. Ricci ^{28, ID}, T. Richert ⁷⁶, M. Richter ^{19, ID},
 W. Riegler ^{32, ID}, F. Riggi ^{26, ID}, C. Ristea ^{63, ID}, M. Rodríguez Cahuantzi ^{44, ID}, K. Røed ^{19, ID}, R. Rogalev ^{142, ID},
 E. Rogochaya ^{143, ID}, T.S. Rogoschinski ^{64, ID}, D. Rohr ^{32, ID}, D. Röhrich ^{20, ID}, P.F. Rojas ⁴⁴, S. Rojas Torres ^{35, ID},
 P.S. Rokita ^{135, ID}, F. Ronchetti ^{48, ID}, A. Rosano ^{30, 52, ID}, E.D. Rosas ⁶⁵, A. Rossi ^{53, ID}, A. Roy ^{47, ID}, P. Roy ¹⁰²,
 S. Roy ^{46, ID}, N. Rubini ^{25, ID}, O.V. Rueda ^{76, ID}, D. Ruggiano ^{135, ID}, R. Rui ^{23, ID}, B. Rumyantsev ¹⁴³,
 P.G. Russek ^{2, ID}, R. Russo ^{85, ID}, A. Rustamov ^{82, ID}, E. Ryabinkin ^{142, ID}, Y. Ryabov ^{142, ID}, A. Rybicki ^{109, ID},
 H. Rytkonen ^{117, ID}, W. Rzesz ^{135, ID}, O.A.M. Saarimaki ^{43, ID}, R. Sadek ^{106, ID}, S. Sadovsky ^{142, ID},
 J. Saetre ^{20, ID}, K. Šafařík ^{35, ID}, S.K. Saha ^{134, ID}, S. Saha ^{81, ID}, B. Sahoo ^{46, ID}, P. Sahoo ⁴⁶, R. Sahoo ^{47, ID},
 S. Sahoo ⁶¹, D. Sahu ^{47, ID}, P.K. Sahu ^{61, ID}, J. Saini ^{134, ID}, K. Sajdakova ³⁷, S. Sakai ^{125, ID}, M.P. Salvan ^{100, ID},
 S. Sambyal ^{92, ID}, T.B. Saramela ¹¹², D. Sarkar ^{136, ID}, N. Sarkar ¹³⁴, P. Sarma ^{41, ID}, V. Sarritzu ^{22, ID},
 V.M. Sarti ^{97, ID}, M.H.P. Sas ^{139, ID}, J. Schambach ^{88, ID}, H.S. Scheid ^{64, ID}, C. Schiaua ^{45, ID}, R. Schicker ^{96, ID},
 A. Schmah ⁹⁶, C. Schmidt ^{100, ID}, H.R. Schmidt ⁹⁵, M.O. Schmidt ^{32, ID}, M. Schmidt ⁹⁵, N.V. Schmidt ^{88, 64, ID},
 A.R. Schmier ^{122, ID}, R. Schotter ^{129, ID}, J. Schukraft ^{32, ID}, K. Schwarz ¹⁰⁰, K. Schweda ^{100, ID}, G. Scioli ^{25, ID},
 E. Scomparin ^{55, ID}, J.E. Seger ^{14, ID}, Y. Sekiguchi ¹²⁴, D. Sekihata ^{124, ID}, I. Selyuzhenkov ^{100, 142, ID},
 S. Senyukov ^{129, ID}, J.J. Seo ^{57, ID}, D. Serebryakov ^{142, ID}, L. Šerkšnytė ^{97, ID}, A. Sevcenco ^{63, ID}, T.J. Shaba ^{68, ID},
 A. Shabanov ¹⁴², A. Shabetai ^{106, ID}, R. Shahoyan ³², W. Shaikh ¹⁰², A. Shangaraev ^{142, ID}, A. Sharma ⁹¹,
 D. Sharma ^{46, ID}, H. Sharma ^{109, ID}, M. Sharma ^{92, ID}, N. Sharma ^{91, ID}, S. Sharma ^{92, ID}, U. Sharma ^{92, ID},
 A. Shatat ^{73, ID}, O. Sheibani ¹¹⁶, K. Shigaki ^{94, ID}, M. Shimomura ⁷⁸, S. Shirinkin ^{142, ID}, Q. Shou ^{39, ID},
 Y. Sibirjak ^{142, ID}, S. Siddhanta ^{51, ID}, T. Siemiarczuk ^{80, ID}, T.F. Silva ^{112, ID}, D. Silvermyr ^{76, ID},
 T. Simantathammakul ¹⁰⁷, R. Simeonov ^{36, ID}, G. Simonetti ³², B. Singh ⁹², B. Singh ^{97, ID}, R. Singh ^{81, ID},
 R. Singh ^{92, ID}, R. Singh ^{47, ID}, V.K. Singh ^{134, ID}, V. Singhal ^{134, ID}, T. Sinha ^{102, ID}, B. Sitar ^{12, ID},
 M. Sitta ^{132, 55, ID}, T.B. Skaali ¹⁹, G. Skorodumovs ^{96, ID}, M. Slupecki ^{43, ID}, N. Smirnov ^{139, ID},

- R.J.M. Snellings ^{59, ID}, E.H. Solheim ^{19, ID}, C. Soncco ¹⁰⁴, J. Song ^{116, ID}, A. Songmoolnak ¹⁰⁷, F. Soramel ^{27, ID}, S. Sorensen ^{122, ID}, R. Spijkers ^{85, ID}, I. Sputowska ^{109, ID}, J. Staa ^{76, ID}, J. Stachel ^{96, ID}, I. Stan ^{63, ID}, P.J. Steffanic ^{122, ID}, S.F. Stiefelmaier ^{96, ID}, D. Stocco ^{106, ID}, I. Storehaug ^{19, ID}, M.M. Storetvedt ^{34, ID}, P. Stratmann ^{137, ID}, S. Strazzi ^{25, ID}, C.P. Stylianidis ⁸⁵, A.A.P. Suaide ^{112, ID}, C. Suire ^{73, ID}, M. Sukhanov ^{142, ID}, M. Suljic ^{32, ID}, V. Sumberia ^{92, ID}, S. Sumowidagdo ^{83, ID}, S. Swain ⁶¹, A. Szabo ¹², I. Szarka ^{12, ID}, U. Tabassam ¹³, S.F. Taghavi ^{97, ID}, G. Taillepied ^{100,127, ID}, J. Takahashi ^{113, ID}, G.J. Tambave ^{20, ID}, S. Tang ^{127,6, ID}, Z. Tang ^{120, ID}, J.D. Tapia Takaki ^{118, ID}, N. Tapus ¹²⁶, L.A. Tarasovicova ^{137, ID}, M.G. Tarzila ^{45, ID}, A. Tauro ^{32, ID}, A. Telesca ^{32, ID}, L. Terlizzi ^{24, ID}, C. Terrevoli ^{116, ID}, G. Tersimonov ³, S. Thakur ^{134, ID}, D. Thomas ^{110, ID}, R. Tieulent ^{128, ID}, A. Tikhonov ^{142, ID}, A.R. Timmins ^{116, ID}, M. Tkacik ¹⁰⁸, T. Tkacik ^{108, ID}, A. Toia ^{64, ID}, N. Topilskaya ^{142, ID}, M. Toppi ^{48, ID}, F. Torales-Acosta ¹⁸, T. Tork ^{73, ID}, A.G. Torres Ramos ^{31, ID}, A. Trifiró ^{30,52, ID}, A.S. Triolo ^{30,52, ID}, S. Tripathy ^{50, ID}, T. Tripathy ^{46, ID}, S. Trogolo ^{32, ID}, V. Trubnikov ^{3, ID}, W.H. Trzaska ^{117, ID}, T.P. Trzcinski ^{135, ID}, R. Turrisi ^{53, ID}, T.S. Tveter ^{19, ID}, K. Ullaland ^{20, ID}, B. Ulukutlu ^{97, ID}, A. Uras ^{128, ID}, M. Urioni ^{54,133, ID}, G.L. Usai ^{22, ID}, M. Vala ³⁷, N. Valle ^{21, ID}, S. Vallero ^{55, ID}, L.V.R. van Doremalen ⁵⁹, M. van Leeuwen ^{85, ID}, C.A. van Veen ^{96, ID}, R.J.G. van Weelden ^{85, ID}, P. Vande Vyvre ^{32, ID}, D. Varga ^{138, ID}, Z. Varga ^{138, ID}, M. Varga-Kofarago ^{138, ID}, M. Vasileiou ^{79, ID}, A. Vasiliev ^{142, ID}, O. Vázquez Doce ^{97, ID}, V. Vechernin ^{142, ID}, E. Vercellin ^{24, ID}, S. Vergara Limón ⁴⁴, L. Vermunt ^{59, ID}, R. Vértesi ^{138, ID}, M. Verweij ^{59, ID}, L. Vickovic ³³, Z. Vilakazi ¹²³, O. Villalobos Baillie ^{103, ID}, G. Vino ^{49, ID}, A. Vinogradov ^{142, ID}, T. Virgili ^{28, ID}, V. Vislavicius ⁸⁴, A. Vodopyanov ^{143, ID}, B. Volkel ^{32, ID}, M.A. Völkl ^{96, ID}, K. Voloshin ¹⁴², S.A. Voloshin ^{136, ID}, G. Volpe ^{31, ID}, B. von Haller ^{32, ID}, I. Vorobyev ^{97, ID}, N. Vozniuk ^{142, ID}, J. Vrláková ^{37, ID}, B. Wagner ²⁰, C. Wang ^{39, ID}, D. Wang ³⁹, M. Weber ^{105, ID}, A. Wegrzynek ^{32, ID}, F.T. Weiglhofer ³⁸, S.C. Wenzel ^{32, ID}, J.P. Wessels ^{137, ID}, S.L. Weyhmiller ^{139, ID}, J. Wiechula ^{64, ID}, J. Wikne ^{19, ID}, G. Wilk ^{80, ID}, J. Wilkinson ^{100, ID}, G.A. Willems ^{137, ID}, B. Windelband ^{96, ID}, M. Winn ^{130, ID}, J.R. Wright ^{110, ID}, W. Wu ³⁹, Y. Wu ^{120, ID}, R. Xu ^{6, ID}, A.K. Yadav ^{134, ID}, S. Yalcin ^{72, ID}, Y. Yamaguchi ^{94, ID}, K. Yamakawa ⁹⁴, S. Yang ²⁰, S. Yano ^{94, ID}, Z. Yin ^{6, ID}, I.-K. Yoo ^{16, ID}, J.H. Yoon ^{57, ID}, S. Yuan ²⁰, A. Yuncu ^{96, ID}, V. Zaccolo ^{23, ID}, C. Zampolli ^{32, ID}, H.J.C. Zanolí ⁵⁹, F. Zanone ^{96, ID}, N. Zardoshti ^{32,103, ID}, A. Zarochentsev ^{142, ID}, P. Závada ^{62, ID}, N. Zaviyalov ¹⁴², M. Zhalov ^{142, ID}, B. Zhang ^{6, ID}, S. Zhang ^{39, ID}, X. Zhang ^{6, ID}, Y. Zhang ¹²⁰, M. Zhao ^{10, ID}, V. Zherebchevskii ^{142, ID}, Y. Zhi ¹⁰, N. Zhigareva ¹⁴², D. Zhou ^{6, ID}, Y. Zhou ^{84, ID}, J. Zhu ^{100,6, ID}, Y. Zhu ⁶, G. Zinovjev ^{3,1}, N. Zurlo ^{133,54, ID}

¹ A.I. Alikhanyan National Science Laboratory (Yerevan Physics Institute) Foundation, Yerevan, Armenia² AGH University of Science and Technology, Cracow, Poland³ Bogolyubov Institute for Theoretical Physics, National Academy of Sciences of Ukraine, Kiev, Ukraine⁴ Bose Institute, Department of Physics and Centre for Astroparticle Physics and Space Science (CAPSS), Kolkata, India⁵ California Polytechnic State University, San Luis Obispo, CA, United States⁶ Central China Normal University, Wuhan, China⁷ Centro de Aplicaciones Tecnológicas y Desarrollo Nuclear (CEADEN), Havana, Cuba⁸ Centro de Investigación y de Estudios Avanzados (CINVESTAV), Mexico City and Mérida, Mexico⁹ Chicago State University, Chicago, IL, United States¹⁰ China Institute of Atomic Energy, Beijing, China¹¹ Chungbuk National University, Cheongju, Republic of Korea¹² Comenius University Bratislava, Faculty of Mathematics, Physics and Informatics, Bratislava, Slovak Republic¹³ COMSATS University Islamabad, Islamabad, Pakistan¹⁴ Creighton University, Omaha, NE, United States¹⁵ Department of Physics, Aligarh Muslim University, Aligarh, India¹⁶ Department of Physics, Pusan National University, Pusan, Republic of Korea¹⁷ Department of Physics, Sejong University, Seoul, Republic of Korea¹⁸ Department of Physics, University of California, Berkeley, CA, United States¹⁹ Department of Physics, University of Oslo, Oslo, Norway²⁰ Department of Physics and Technology, University of Bergen, Bergen, Norway²¹ Dipartimento di Fisica, Università di Pavia, Pavia, Italy²² Dipartimento di Fisica dell'Università and Sezione INFN, Cagliari, Italy²³ Dipartimento di Fisica dell'Università and Sezione INFN, Trieste, Italy²⁴ Dipartimento di Fisica dell'Università and Sezione INFN, Turin, Italy

- ²⁵ Dipartimento di Fisica e Astronomia dell'Università and Sezione INFN, Bologna, Italy
²⁶ Dipartimento di Fisica e Astronomia dell'Università and Sezione INFN, Catania, Italy
²⁷ Dipartimento di Fisica e Astronomia dell'Università and Sezione INFN, Padova, Italy
²⁸ Dipartimento di Fisica 'E.R. Caianiello' dell'Università and Gruppo Collegato INFN, Salerno, Italy
²⁹ Dipartimento DISAT del Politecnico and Sezione INFN, Turin, Italy
³⁰ Dipartimento di Scienze MIFT, Università di Messina, Messina, Italy
³¹ Dipartimento Interateneo di Fisica 'M. Merlin' and Sezione INFN, Bari, Italy
³² European Organization for Nuclear Research (CERN), Geneva, Switzerland
³³ Faculty of Electrical Engineering, Mechanical Engineering and Naval Architecture, University of Split, Split, Croatia
³⁴ Faculty of Engineering and Science, Western Norway University of Applied Sciences, Bergen, Norway
³⁵ Faculty of Nuclear Sciences and Physical Engineering, Czech Technical University in Prague, Prague, Czech Republic
³⁶ Faculty of Physics, Sofia University, Sofia, Bulgaria
³⁷ Faculty of Science, P.J. Šafárik University, Košice, Slovak Republic
³⁸ Frankfurt Institute for Advanced Studies, Johann Wolfgang Goethe-Universität Frankfurt, Frankfurt, Germany
³⁹ Fudan University, Shanghai, China
⁴⁰ Gangneung-Wonju National University, Gangneung, Republic of Korea
⁴¹ Gauhati University, Department of Physics, Guwahati, India
⁴² Helmholtz-Institut für Strahlen- und Kernphysik, Rheinische Friedrich-Wilhelms-Universität Bonn, Bonn, Germany
⁴³ Helsinki Institute of Physics (HIP), Helsinki, Finland
⁴⁴ High Energy Physics Group, Universidad Autónoma de Puebla, Puebla, Mexico
⁴⁵ Horia Hulubei National Institute of Physics and Nuclear Engineering, Bucharest, Romania
⁴⁶ Indian Institute of Technology Bombay (IIT), Mumbai, India
⁴⁷ Indian Institute of Technology Indore, Indore, India
⁴⁸ INFN, Laboratori Nazionali di Frascati, Frascati, Italy
⁴⁹ INFN, Sezione di Bari, Bari, Italy
⁵⁰ INFN, Sezione di Bologna, Bologna, Italy
⁵¹ INFN, Sezione di Cagliari, Cagliari, Italy
⁵² INFN, Sezione di Catania, Catania, Italy
⁵³ INFN, Sezione di Padova, Padova, Italy
⁵⁴ INFN, Sezione di Pavia, Pavia, Italy
⁵⁵ INFN, Sezione di Torino, Turin, Italy
⁵⁶ INFN, Sezione di Trieste, Trieste, Italy
⁵⁷ Inha University, Incheon, Republic of Korea
⁵⁸ Institute for Advanced Simulation, Forschungszentrum Jülich, Jülich, Germany
⁵⁹ Institute for Gravitational and Subatomic Physics (GRASP), Utrecht University/Nikhef, Utrecht, Netherlands
⁶⁰ Institute of Experimental Physics, Slovak Academy of Sciences, Košice, Slovak Republic
⁶¹ Institute of Physics, Homi Bhabha National Institute, Bhubaneswar, India
⁶² Institute of Physics of the Czech Academy of Sciences, Prague, Czech Republic
⁶³ Institute of Space Science (ISS), Bucharest, Romania
⁶⁴ Institut für Kernphysik, Johann Wolfgang Goethe-Universität Frankfurt, Frankfurt, Germany
⁶⁵ Instituto de Ciencias Nucleares, Universidad Nacional Autónoma de México, Mexico City, Mexico
⁶⁶ Instituto de Física, Universidade Federal do Rio Grande do Sul (UFRGS), Porto Alegre, Brazil
⁶⁷ Instituto de Física, Universidad Nacional Autónoma de México, Mexico City, Mexico
⁶⁸ iThemba LABS, National Research Foundation, Somerset West, South Africa
⁶⁹ Jeonbuk National University, Jeonju, Republic of Korea
⁷⁰ Johann-Wolfgang-Goethe Universität Frankfurt Institut für Informatik, Fachbereich Informatik und Mathematik, Frankfurt, Germany
⁷¹ Korea Institute of Science and Technology Information, Daejeon, Republic of Korea
⁷² KTO Karatay University, Konya, Turkey
⁷³ Laboratoire de Physique des 2 Infinis, Irène Joliot-Curie, Orsay, France
⁷⁴ Laboratoire de Physique Subatomique et de Cosmologie, Université Grenoble-Alpes, CNRS-IN2P3, Grenoble, France
⁷⁵ Lawrence Berkeley National Laboratory, Berkeley, CA, United States
⁷⁶ Lund University Department of Physics, Division of Particle Physics, Lund, Sweden
⁷⁷ Nagasaki Institute of Applied Science, Nagasaki, Japan
⁷⁸ Nara Women's University (NWU), Nara, Japan
⁷⁹ National and Kapodistrian University of Athens, School of Science, Department of Physics, Athens, Greece
⁸⁰ National Centre for Nuclear Research, Warsaw, Poland
⁸¹ National Institute of Science Education and Research, Homi Bhabha National Institute, Jatni, India
⁸² National Nuclear Research Center, Baku, Azerbaijan
⁸³ National Research and Innovation Agency – BRIN, Jakarta, Indonesia
⁸⁴ Niels Bohr Institute, University of Copenhagen, Copenhagen, Denmark
⁸⁵ Nikhef, National institute for subatomic physics, Amsterdam, Netherlands
⁸⁶ Nuclear Physics Group, STFC Daresbury Laboratory, Daresbury, United Kingdom
⁸⁷ Nuclear Physics Institute of the Czech Academy of Sciences, Husinec-Řež, Czech Republic
⁸⁸ Oak Ridge National Laboratory, Oak Ridge, TN, United States
⁸⁹ Ohio State University, Columbus, OH, United States
⁹⁰ Physics department, Faculty of science, University of Zagreb, Zagreb, Croatia
⁹¹ Physics Department, Panjab University, Chandigarh, India
⁹² Physics Department, University of Jammu, Jammu, India
⁹³ Physics Department, University of Rajasthan, Jaipur, India
⁹⁴ Physics Program and International Institute for Sustainability with Knotted Chiral Meta Matter (SKCM2), Hiroshima University, Hiroshima, Japan
⁹⁵ Physikalisches Institut, Eberhard-Karls-Universität Tübingen, Tübingen, Germany
⁹⁶ Physikalisches Institut, Ruprecht-Karls-Universität Heidelberg, Heidelberg, Germany
⁹⁷ Physik Department, Technische Universität München, Munich, Germany
⁹⁸ Politecnico di Bari and Sezione INFN, Bari, Italy
⁹⁹ Research Center for Nuclear Physics, Osaka University, Osaka, Japan
¹⁰⁰ Research Division and ExtreMe Matter Institute EMMI, GSI Helmholtzzentrum für Schwerionenforschung GmbH, Darmstadt, Germany
¹⁰¹ RIKEN iTHEMS, Wako, Japan
¹⁰² Saha Institute of Nuclear Physics, Homi Bhabha National Institute, Kolkata, India
¹⁰³ School of Physics and Astronomy, University of Birmingham, Birmingham, United Kingdom
¹⁰⁴ Sección Física, Departamento de Ciencias, Pontificia Universidad Católica del Perú, Lima, Peru

- ¹⁰⁵ Stefan Meyer Institut für Subatomare Physik (SMI), Vienna, Austria
¹⁰⁶ SUBATECH, IMT Atlantique, Nantes Université, CNRS-IN2P3, Nantes, France
¹⁰⁷ Suranaree University of Technology, Nakhon Ratchasima, Thailand
¹⁰⁸ Technical University of Košice, Košice, Slovak Republic
¹⁰⁹ The Henryk Niewodniczanski Institute of Nuclear Physics, Polish Academy of Sciences, Cracow, Poland
¹¹⁰ The University of Texas at Austin, Austin, TX, United States
¹¹¹ Universidad Autónoma de Sinaloa, Culiacán, Mexico
¹¹² Universidade de São Paulo (USP), São Paulo, Brazil
¹¹³ Universidade Estadual de Campinas (UNICAMP), Campinas, Brazil
¹¹⁴ Universidade Federal do ABC, Santo Andre, Brazil
¹¹⁵ University of Cape Town, Cape Town, South Africa
¹¹⁶ University of Houston, Houston, TX, United States
¹¹⁷ University of Jyväskylä, Jyväskylä, Finland
¹¹⁸ University of Kansas, Lawrence, KS, United States
¹¹⁹ University of Liverpool, Liverpool, United Kingdom
¹²⁰ University of Science and Technology of China, Hefei, China
¹²¹ University of South-Eastern Norway, Kongsberg, Norway
¹²² University of Tennessee, Knoxville, TN, United States
¹²³ University of the Witwatersrand, Johannesburg, South Africa
¹²⁴ University of Tokyo, Tokyo, Japan
¹²⁵ University of Tsukuba, Tsukuba, Japan
¹²⁶ University Politehnica of Bucharest, Bucharest, Romania
¹²⁷ Université Clermont Auvergne, CNRS/IN2P3, LPC, Clermont-Ferrand, France
¹²⁸ Université de Lyon, CNRS/IN2P3, Institut de Physique des 2 Infinis de Lyon, Lyon, France
¹²⁹ Université de Strasbourg, CNRS, IPHC UMR 7178, F-67000 Strasbourg, France
¹³⁰ Université Paris-Saclay Centre d'Etudes de Saclay (CEA), IRFU, Département de Physique Nucléaire (DPhN), Saclay, France
¹³¹ Università degli Studi di Foggia, Foggia, Italy
¹³² Università del Piemonte Orientale, Vercelli, Italy
¹³³ Università di Brescia, Brescia, Italy
¹³⁴ Variable Energy Cyclotron Centre, Homi Bhabha National Institute, Kolkata, India
¹³⁵ Warsaw University of Technology, Warsaw, Poland
¹³⁶ Wayne State University, Detroit, MI, United States
¹³⁷ Westfälische Wilhelms-Universität Münster, Institut für Kernphysik, Münster, Germany
¹³⁸ Wigner Research Centre for Physics, Budapest, Hungary
¹³⁹ Yale University, New Haven, CT, United States
¹⁴⁰ Yonsei University, Seoul, Republic of Korea
¹⁴¹ Zentrum für Technologie und Transfer (ZTT), Worms, Germany
¹⁴² Affiliated with an institute covered by a cooperation agreement with CERN
¹⁴³ Affiliated with an international laboratory covered by a cooperation agreement with CERN

^I Deceased.^{II} Also at: Max-Planck-Institut für Physik, Munich, Germany.^{III} Also at: Italian National Agency for New Technologies, Energy and Sustainable Economic Development (ENEA), Bologna, Italy.^{IV} Also at: Dipartimento DET del Politecnico di Torino, Turin, Italy.^V Also at: Department of Applied Physics, Aligarh Muslim University, Aligarh, India.^{VI} Also at: Institute of Theoretical Physics, University of Wroclaw, Poland.^{VII} Also at: An institution covered by a cooperation agreement with CERN.